

A comparison between two pneumatic suspension architectures

*Original*

A comparison between two pneumatic suspension architectures / Quaglia, Giuseppe; Scopesi, Marco; Franco, Walter. - In: VEHICLE SYSTEM DYNAMICS. - ISSN 0042-3114. - STAMPA. - 50:4(2012), pp. 509-526. [10.1080/00423114.2011.602420]

*Availability:*

This version is available at: 11583/2486998 since:

*Publisher:*

TAYLOR & FRANCIS LTD

*Published*

DOI:10.1080/00423114.2011.602420

*Terms of use:*

This article is made available under terms and conditions as specified in the corresponding bibliographic description in the repository

*Publisher copyright*

(Article begins on next page)

# A comparison between two pneumatic suspension architectures

G. Quaglia\*, M. Scopesi and W. Franco

*Politecnico di Torino, Dipartimento di Meccanica, Turin, Corso Duca degli Abruzzi 24, Italy*

The aim of this work is to assess and compare the mathematical models of two pneumatic suspension architectures and show how they can converge, after appropriate simplifications, to a general linear form. After making this model dimensionless, it will be used to study, with a transmissibility analysis, the behaviour of a mono-suspension (quarter-car model). Finally, an example of a design process will be shown to highlight the strengths and weaknesses of both architectures and to provide the reader with a practical design tool.

**Keywords:** air spring; pneumatic suspension; optimisation

## 1. Introduction

Vehicular suspensions must fulfil two main tasks. First, they have to ensure the active safety by correctly redistributing the forces exchanged between the tyres and road, thus ensuring the general road-holding of the vehicle itself. Secondly, they have to ensure the comfort of the passengers by filtering, as far as possible, the road roughness. Since these two aspects are mutually conflicting, in recent decades there has been considerable effort from the scientific community and manufacturers, in the study of advanced suspensions for ground vehicles. This interest is reflected in [1], where it is possible to find over 500 references prior to 1995, related to this topic and grouped into several categories. They range from the optimisation of passive, semi-active or active suspensions to the modelling of soil–tyre contact and vehicle dynamics.

For what concerns vehicular suspensions, an important branch of study, which is also the subject of this work, is the air suspensions field that can be found associated with active, semi-active or passive devices. They are especially used as a self-levelling system for commercial vehicles (trucks, trains, etc.), which require that the static height of the carbody is kept constant, even with strong paying load variations. The most commonly used type is certainly the air spring, in which mass changes are counterbalanced by inner pressure, keeping the static height of the vehicle, as well as its natural frequency, more or less constant. Besides this advantage, they are usually lighter than a mechanical springs, especially of those with low stiffness and large static force (strong precompression).

The air springs are recently used also in small commercial vehicles or sport utility vehicles (SUVs) where the load variations are still significant, commonly paired with traditional hydraulic dampers: it is possible to cite the Volkswagen [2], the Audi [3] or the Porsche [4]. This approach, however, frustrates some positive aspects that could be obtained by using a pneumatic damper, such as better insulation to vibration frequencies in the range between 4 and 8 Hz, to which, according to ISO 2631, the human body is most sensitive. For these reasons, there are numerous studies in the literature in which the air springs are coupled with pneumatic dampers.

The most commonly used layout is obtained by connecting the chamber of an air spring with a fixed auxiliary external volume by means of a fluidic resistance: this way, the damping effect due to the transfer of air between the two volumes is added to the stiffness due to air compression. This type of architecture is present in the literature since 1961 [5] and is used, generally coupled with a laminar resistance, to obtain linearised models easily as in [6] or more recently in [7]. From these studies, it is clear that, in order to minimise vibrations from the road to the sprung mass, it is necessary to have a great ratio between the outer chamber's volume and the air spring's volume, thus leading to a bulky solution. To partially overcome this problem, in [8] the effect of the connecting pipe has been studied in more detail using a finite-difference model, to understand when it is feasible to move the auxiliary volume away from the wheel where, possibly, there is more space.

The use of linear mathematical models allows us to obtain simple equations from which, if properly handled, more significant information can be extracted. Quaglia and Sorli [9] and later Nieto *et al.* [7] have developed a linear dimensionless model of the classical air suspension architecture, which shows that, as already said, the key parameter to soften the maximum in the transmissibility curve is the ratio between the auxiliary volume and the spring's volume and that the fluidic resistance has no effect on this peak. This can lead to the obvious problem of spaces, especially if the suspension is applied to relatively small vehicles.

The focus of this work is on passive air suspension systems, which, the authors believe, have still great advantages in simplicity, lightweight and reliability over active solutions. The purpose of this work is to find a general procedure to design a passive air suspension, which also takes into account the practical issues such as spaces. To achieve this goal, the classic air spring with auxiliary volume will be compared with a less bulky layout using a common dimensionless model, whose parameters differ for the two layouts. Using this model, both suspensions will be sized for the same application to highlight, from a practical point of view, the advantages and disadvantages of both. Since the main focus will be on ride comfort and as the most critical frequencies are, according to the ISO2631, up to 8–10 Hz, a simple model with two degrees of freedom will be used, thus without taking into account the effect of tyres, which is not negligible at higher frequencies.

The main contributions of this work are a comparison between the two mentioned architectures using linear dimensionless models and the development of a design process that highlights the strengths and weaknesses of both systems and provides the reader with a practical design tool.

## 2. Description of the two architectures

Both suspension architectures introduced here (Figure 1) are passive, but they also have a device, not shown in any figure, which is able to statically adjust the internal pressure in order to adapt it to mass changes or to a different required static height. To show their working principles in a simple, yet realistic way, rigid pneumatic cylinders, instead of air springs, will be used: this is justified since the linearised behaviour of an rolling diaphragm air spring around its initial condition may be the same of a fixed-area pneumatic cylinder.

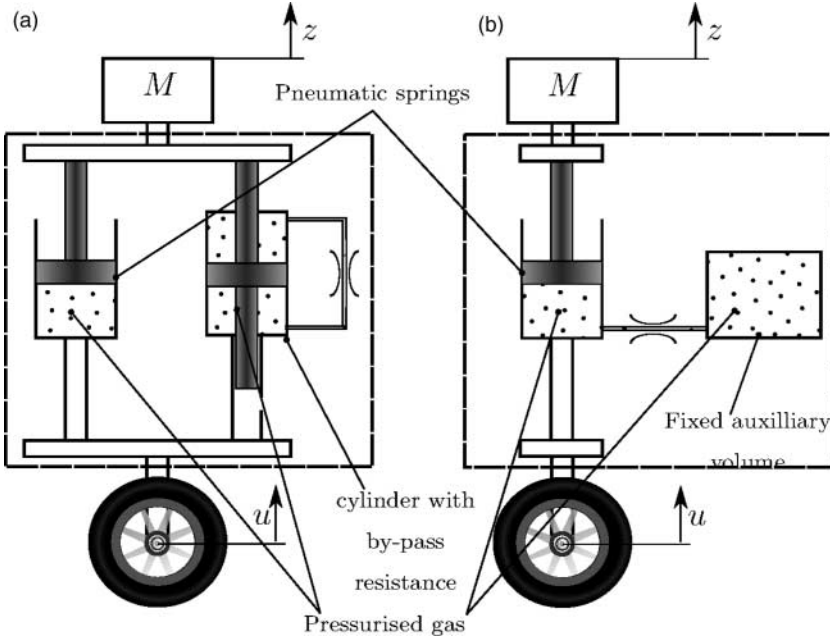


Figure 1. (a) BPR and (b) FAV suspension systems.

### 2.1. *Pneumatic suspension with by-pass resistance*

This device is composed of two cylinders: the first, which is a simple effect one, represents the pneumatic spring needed to provide the requested static force and the desired static stiffness. The second, thanks to a fluidic resistance connecting its chambers, is used to obtain a damping effect. The static height can be kept constant adjusting the pressure level of the first cylinder, while the pressure level in the second cylinder can be used to independently increase or decrease the damping effect.

### 2.2. *Pneumatic suspension with fixed auxiliary volume*

This is the classic air suspension architecture which has been already cited in the introduction, and since it is widespread in literature, it will be used as a reference. It is composed of a simple-effect cylinder (pneumatic spring) connected to an auxiliary volume by means of a fluidic resistance. The static height is kept constant by adjusting the air pressure level in the system, thus consequently changing the stiffness and the damping effect as well.

## 3. Suspension models

### 3.1. *Basic models*

Two basic mathematical models are required to analyse both by-pass resistance (BPR) and fixed auxiliary volume (FAV) suspension systems, one representing a variable volume with one air inlet and the other representing the fluidic resistance. In the following, nonlinear and linear models are defined and, by properly composing them, it is possible to write the equations for BPR or FAV.

### 3.1.1. Volume with one inlet: nonlinear model

Figure 2 shows a sketch of a variable volume chamber with one inlet. The dashed line contains the control volume which is the portion of space under study. This is useful for modelling the air inside all cylinders as well as the auxiliary reservoir of the FAV suspension system.

Using the mass conservation principle for the volume in Figure 2:

$$G_{in} = \frac{dm}{dt} = \frac{d}{dt}(\rho V) = \frac{d\rho}{dt}V + \frac{dV}{dt}\rho. \quad (1)$$

Using the perfect gas state equation and imposing a reversible adiabatic process inside the control volume, the following expression for the pressure–time derivative is obtained:

$$\frac{dP}{dt} = -\frac{\gamma AP}{V_0 + Ay}\dot{y} + \frac{\gamma R_g T_0}{V_0 + Ay} \left( \frac{P}{P_0} \right)^{(\gamma-1)/\gamma} G_{in}. \quad (2)$$

### 3.1.2. Volume with one inlet: linear model

Linearising Equation (2) around the following initial conditions:

$$P = P_0; \quad \frac{dP}{dt} = 0; \quad y = 0; \quad \dot{y} = 0; \quad G_{in} = 0, \quad (3)$$

and transforming according to Laplace, the following linear model is obtained:

$$\bar{P} - \frac{P_0}{s} = -\frac{\gamma AP_0}{V_0} \bar{y} + \frac{\gamma R_g T_0}{V_0} \bar{G}_{in}. \quad (4)$$

This is the expression used in the following sections to deal with volume, being variable, as a cylinder's chamber, or being fixed, as an external reservoir.

The equilibrium of the piston in Figure 2 is:

$$F + F_0 = (P - P_{atm})A, \quad (5)$$

where the static force is  $F_0 = (P_0 - P_{atm})A$  and the dynamic force is  $F = (P - P_0)A$ , whose Laplace transform is:

$$\bar{F} = \left( \bar{P} - \frac{P_0}{s} \right) A. \quad (6)$$

### 3.1.3. Fluidic resistance

The fluidic resistance can be considered to be an orifice or a thin pipe: in the former case, the flow is mainly turbulent while in the latter it is laminar.

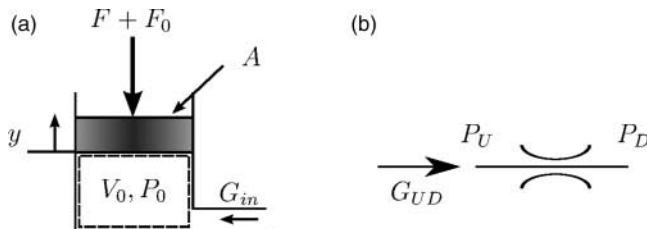


Figure 2. (a) Variable volume chamber with one inlet and (b) fluidic resistance.

3.1.3.1. *Orifice: nonlinear model.* The flow through an orifice can be modelled in accordance with ISO 6358:

$$\begin{aligned} G_{UD} &= CP_U \rho_{ANR} \sqrt{\frac{T_{ANR}}{T_U}} & \text{if } 0 \leq \frac{P_D}{P_U} \leq b, \\ G_{UD} &= CP_U \rho_{ANR} \sqrt{\frac{T_{ANR}}{T_U}} \sqrt{1 - \left( \frac{P_U/P_D - b}{1 - b} \right)^2} & \text{if } 1 \geq \frac{P_D}{P_U} > b, \end{aligned} \quad (7)$$

where  $T_{ANR}$  and  $\rho_{ANR}$  are the temperature and the density of the air at standard conditions, pressure  $P_U$  (pressure upstream) is greater than  $P_D$  (pressure downstream) (Figure 2),  $b$  is the critical pressure ratio,  $C$  is the sonic conductance of the orifice and  $T_U$  is the upstream temperature. Since these equations are strongly nonlinear, it is not very reliable to use a linearised model. However, there are works in which this behaviour has been linearised using a variable opening orifice, such as [10].

3.1.3.2. *Narrow pipe: nonlinear model.* The laminar flow through a narrow pipe can be modelled as Equation (4.37) in [11]:

$$G = \rho \frac{\pi D^4}{128 \mu L} (P_U - P_D), \quad (8)$$

where  $L$  is the pipe length,  $\mu$  is the viscosity of the air,  $D$  is the diameter of the pipe and  $P_U$  and  $P_D$  are the upstream and downstream pressure as before. In a compressible fluid like air, the density  $\rho$  is not a constant; however, the behaviour of this kind of pipe, unlike the orifice, is reasonably approximated to be linear. This model does not take into account any inertial effect of the air, which, according to [8], could not be negligible.

3.1.3.3. *Linear model.* A simple linear model, with  $G_{UD0} = 0$ , will be considered in the following for the fluidic resistance:

$$\bar{G}_{UD} = \frac{\bar{P}_U - \bar{P}_D}{R}. \quad (9)$$

For the specific aim of this work, it does not matter if this model derives from the orifice or the narrow pipe because there are no further investigations on the design of the resistance itself.

### 3.2. BPR linear model

Looking at Figure 3, the force on the upper plate can be divided in two parts, one for each cylinder. First, the forces related to each one of them will be obtained and then they will be added to obtain the total force.

#### 3.2.1. Damper

Using Equation (4) for chamber A ( $x \equiv y$  and  $G_{AB} \equiv -G_{in}$ ) and B ( $x \equiv -y$  and  $G_{AB} \equiv G_{in}$ ), Equation (9) for the mass flow rate and Equation (6) for the piston equilibrium, the following



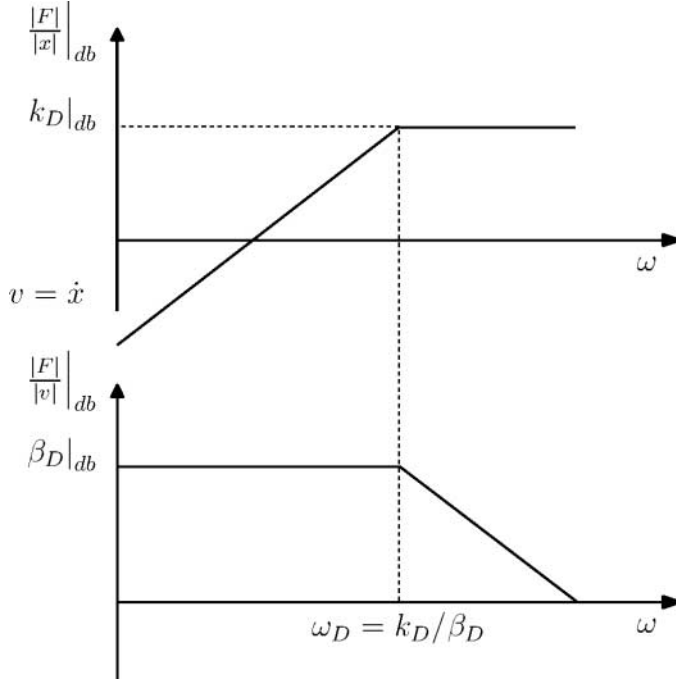


Figure 4. Transfer function of Equation (11).

between the two chambers is negligible and the device behaves like a spring. The parameter  $\beta_D$  has the dimension of a damping coefficient ( $\text{N s m}^{-1}$ ) and expresses the ratio between force and velocity ( $|F|/|v|$ ) at a low frequency. Finally, the frequency  $\omega_D$  delimits the two cited regions (functioning as spring and as damper), as shown in Figure 4. Of those three parameters, just two can be independently chosen.

### 3.2.2. Stiffness

The chamber of the first actuator (Figure 3) is isolated and so, by changing its initial pressure, the stiffness can be changed accordingly. Using Equations (4) (with  $G_{in} = 0$  and  $x \equiv y$ ) and (6), the expression of the dynamic force is obtained:

$$\bar{F}_S = -\frac{\gamma A_S^2 P_{S0}}{V_{S0}} \bar{x} = -k_S \bar{x}. \quad (13)$$

The parameter  $k_S$  is the ratio between the force and the deformation ( $|F|/|x|$ ) of the actuator S and so, it is the stiffness of the actuator itself.

### 3.2.3. Total force

The equilibrium of the plate of BPR suspension is, according to Figure 3:

$$F + F_0 = F_S + F_{S0} + F_D, \quad (14)$$

where in the static condition, the equation simplify to:

$$F_0 = F_{S0} = (P_{S0} - P_{atm})A_S = Mg. \quad (15)$$



The dynamic force is instead computed by summing Equations (13) and (11):

$$\bar{F} = -k_S \frac{s\beta_D((k_D + k_S)/k_D k_S) + 1}{s(\beta_D/k_D) + 1} \bar{x} = -k_S \frac{s/\omega_{SD} + 1}{s/\omega_D + 1} \bar{x}, \quad (16)$$

where

$$\omega_{SD} = \frac{k_S}{k_S + k_D} \omega_D = \frac{2\gamma R_g T_{D0} A_S^2 P_{S0}}{R(V_{D0} A_S^2 P_{S0} + 2V_{S0} A_D^2 P_{D0})}. \quad (17)$$

Figure 5 shows the magnitude, in decibel, of the complete BPR device ( $\bar{F}/\bar{x}$ ).

The two highlighted frequencies,  $\omega_{SD}$  and  $\omega_D$ , divide the axis into three regions: a central part where the device behaves like a damper and two external parts where it behaves like a spring, whose stiffness increases from  $k_S$  to  $k_S + k_D$ . Since  $\omega_{SD} < \omega_D$ , there are three free parameters to design a BPR suspension.

### 3.3. FAV linear model

Applying Equations (4) and (6) with  $y \equiv x$ ,  $G_{in} \equiv -G_{SA}$  and  $P_{S0} = P_{A0} = P_0$  to the spring  $S$  in Figure 6, the following equation can be obtained:

$$\bar{F} = \left( \bar{P}_S - \frac{P_0}{s} \right) A_S = -\frac{\gamma P_0 A_S^2}{V_{S0}} \bar{x} - \frac{\gamma A_S R_g T_0}{V_{S0}} \frac{\bar{G}_{SA}}{s}. \quad (18)$$

Applying Equation (4) to the auxiliary volume  $A$ , with  $y \equiv 0$  and  $G_{in} \equiv G_{SA}$ , brings:

$$\bar{P}_A - \frac{P_0}{s} = \frac{\gamma R_g T_0}{V_{A0}} \frac{\bar{G}_{SA}}{s}. \quad (19)$$

From Equation (9), instead, we derive the mass flow rate:

$$\bar{G}_{SA} = \frac{\bar{P}_S - \bar{P}_A}{R}. \quad (20)$$

Solving this system of equations, the following transfer function can be obtained:

$$\frac{\bar{F}}{\bar{x}} = -\frac{\gamma P_0 A_S}{V_{S0} + V_{A0}} \cdot \frac{(RV_{A0}/\gamma R_g T_0)s + 1}{(RV_{A0}/\gamma R_g T_0) \cdot (V_{S0}/(V_{S0} + V_{A0}))s + 1}. \quad (21)$$

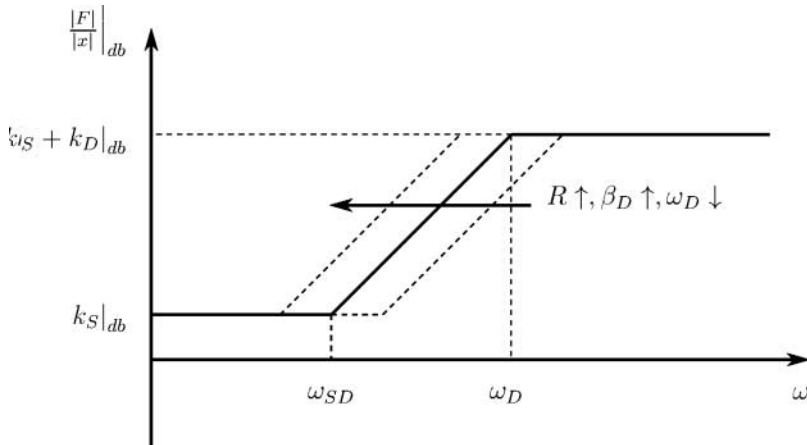


Figure 5. BPR transfer function.



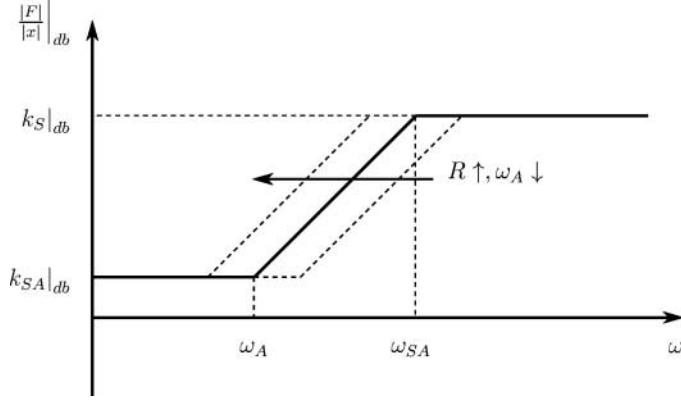


Figure 7. FAV transfer function.

- The pole defining the end of the damping behaviour is  $\omega_D$  for BPR and it is the function of only the damper while, for FAV, it is  $\omega_{SA}$ , function of parameters from the spring and the auxiliary volume.

#### 4. Quarter-car model

Figure 8 shows the quarter-car model of a generic suspension system, where tyre strain has been neglected. Statically, the equilibrium is simply  $F_0 = Mg$ , while the dynamic equilibrium is  $m\ddot{z} = F$ . From this dynamic equation, it is possible to write a quarter-car model for both BPR and FAV:

BPR

$$Ms^2\bar{z} = \bar{F} = -k_S \frac{s/\omega_{SD} + 1}{s/\omega_D + 1} (\bar{z} - \bar{u}),$$

$$\frac{\bar{z}}{\bar{u}} = \frac{s/\omega_{SD} + 1}{s^3/(\omega_D^2\omega_{nB}^2) + s^2/\omega_{nB}^2 + s/\omega_{SD} + 1}$$

FAV

$$Ms^2\bar{z} = \bar{F} = -k_{SA} \frac{s/\omega_A + 1}{s/\omega_{SA} + 1} (\bar{z} - \bar{u}), \quad (25)$$

$$\frac{\bar{z}}{\bar{u}} = \frac{s/\omega_A + 1}{s^3/(\omega_{SA}^2\omega_{nF}^2) + s^2/\omega_{nF}^2 + s/\omega_A + 1}, \quad (26)$$

where  $\omega_{nB} = \sqrt{k_S/M}$  and  $\omega_{nF} = \sqrt{k_{SA}/M}$ .

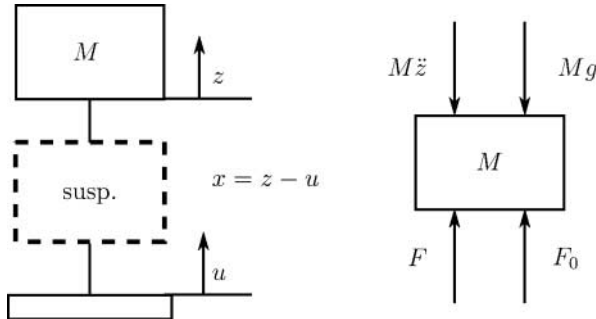


Figure 8. Quarter-car model free body diagram.

#### 4.1. Dimensionless quarter-car model

Since the two models are formally equivalent, it is possible to develop a common dimensionless transmissibility function:

$$H(s) = \frac{\bar{z}}{\bar{u}} = \frac{\psi \lambda (s/\omega_n) + 1}{\psi (s/\omega_n)^3 + (s/\omega_n)^2 + \psi \lambda (s/\omega_n) + 1}, \quad (27)$$

where  $\omega_n$  is the natural frequency  $\omega_{nB}$  or  $\omega_{nF}$ . Table 1 summarises, for both BPR and FAV suspensions, the expressions of  $\omega_n$ ,  $\psi$  and  $\lambda$ , obtained by comparing the generic quarter-car dimensionless model of Equation (27) with the specific model of Equation (26) and also introduces the dimensionless frequency  $\chi$ .

The parameter  $\psi$  is mainly controlled from the pneumatic resistance  $R$  and there are the following particular cases: for  $R \rightarrow 0$  ( $\psi \rightarrow 0$ ), all volumes are connected without the damping effect, and the transfer function (27) becomes a second-order system with natural frequency  $\omega_n$  and without damping:

$$H(s) \simeq \frac{1}{(s^2/\omega_n^2) + 1}. \quad (28)$$

On the other hand, if  $R \rightarrow \infty$  ( $\psi \rightarrow \infty$ ), all volumes are separated, again without any damping effect, leading to a transfer function with natural frequency  $\omega_n \sqrt{\lambda}$ :

$$H(s) \simeq \frac{\psi \lambda (s/\omega_n)}{\psi (s/\omega_n)^3 + \psi \lambda (s/\omega_n)} = \frac{1}{(1/\lambda)(s/\omega_n)^2 + 1}. \quad (29)$$

It follows that the distance between these two extreme behaviours is the function of  $\lambda$  alone (Figure 9), and, referring to Table 1, it can be adjusted for an FAV system, only with the volumes ratio, while for BPR, also with the pressures and the areas, gaining more freedom during the design.

To obtain an analytical expression of the ratio between the module of chassis displacement and the module of the tyre displacement, given a sinusoidal input ( $u = u_0 \sin \omega t$ ), the module of  $H(j\chi)$  is needed, since:

$$\frac{|z_0 \sin \omega t|}{|u_0 \sin \omega t|} = \frac{z_0}{u_0} = |H(j\chi)|. \quad (30)$$

Table 1. Suspension's parameters.

	BPR	FAV
$\omega_n$	$\omega_{nB} = \sqrt{\frac{k_S}{M}} = \sqrt{\frac{\gamma A_S^2 P_{S0}}{M V_{S0}}}$	$\omega_{nF} = \sqrt{\frac{k_{SA}}{M}} = \sqrt{\frac{\gamma A_S^2 P_0}{M(V_{S0} + V_{A0})}}$
$\psi$	$\frac{\omega_{nB}}{\omega_D} = \frac{R V_{D0}}{2 \gamma R_g T_{D0}} \sqrt{\frac{\gamma A_S^2 P_{S0}}{M V_{S0}}}$	$\frac{\omega_{nF}}{\omega_{SA}} = \frac{R V_{A0} V_{S0}}{\gamma R_g T_0 (V_{S0} + V_{A0})} \sqrt{\frac{\gamma A_S^2 P_0}{M(V_{S0} + V_{A0})}}$
$\lambda$	$\frac{\omega_D}{\omega_{SD}} = 1 + 2 \frac{V_{S0} P_{D0} A_D^2}{V_{D0} P_{S0} A_S^2}$	$\frac{\omega_{SA}}{\omega_A} = 1 + \frac{V_{A0}}{V_{S0}}$
$\chi$	$\frac{\omega}{\omega_{nB}} = \omega \sqrt{\frac{M V_{S0}}{\gamma A_S^2 P_{S0}}}$	$\frac{\omega}{\omega_{nF}} = \omega \sqrt{\frac{M(V_{S0} + V_{A0})}{\gamma A_S^2 P_0}}$

And then the module of  $H(j\chi)$  is:

$$\begin{aligned} |H(j\chi)| &= \sqrt{\frac{1 + (\psi\lambda\chi)^2}{(1 - \chi^2)^2 + \chi^2(\psi\lambda - \psi\chi^2)^2}}, \\ &= \frac{1}{|1 - \chi^2|} \sqrt{\frac{1 + (\psi\lambda\chi)^2}{1 + (\chi\psi)^2((\lambda - \chi^2)/(1 - \chi^2))^2}}. \end{aligned} \quad (31)$$

It is worth to notice the following property of this transfer function: if  $((\lambda - \chi^2)/(1 - \chi^2))^2 = \lambda^2$ , the term under the square root is one, leading to a specific value of  $\chi$  and  $H$ :

$$\chi^* = \sqrt{\frac{2\lambda}{\lambda + 1}}; \quad H^* = \frac{\lambda + 1}{\lambda - 1}. \quad (32)$$

Since the  $\chi^*, H^*$  coordinate do not depend on  $\psi$ , it is a common point for all curves regardless of the actual value of the parameter  $\psi$ . The effect of increasing  $\lambda$  is, apart from the growing of the distance between the two peaks in Figure 9, the lowering of the intersection point  $H^*$  (up to a minimum of 1), as shown by Equation (32). Looking at Figure 9, it is clear that there is a specific value of  $\psi$  whose maximum is  $H^*$ : this transmissibility curve, from the point of view of the ride comfort, represents an optimum, since it has the lowest peak. To find it, it is necessary to calculate the value of  $\psi$  which nullifies the derivative of  $|H(j\chi)|$  in  $\chi^*$ , that is:

$$\psi^* = \sqrt{\frac{\lambda + 1}{2\lambda^2}}. \quad (33)$$

With this condition,  $\psi$  is not a free parameter during the design process, but just a consequence of  $\lambda$  and of the chosen optimisation.

From Equation (27), it follows that  $\lambda$ ,  $\psi$  and  $\omega_n$  are the only parameters affecting the quarter-car model. While the first two are dimensionless,  $\omega_n$  has the dimension of a frequency ( $\text{rad s}^{-1}$ ), since it depends on the ratio between the static stiffness and the mass and defines the position of  $|H(j\chi)|$  in the frequency axis.

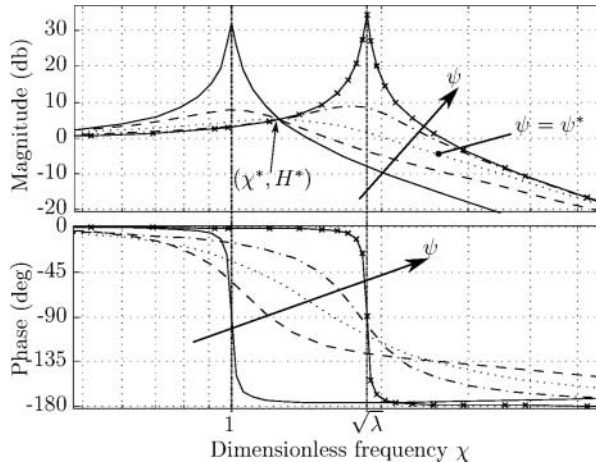


Figure 9. Module and phase of  $H(j\chi)$  with  $\lambda = 3.5$ .

## 4.2. Mass changes

It is desirable to have a suspension whose dynamical behaviour is independent of the sprung mass and also with a constant static height. To achieve this, the three mentioned parameters  $\lambda$ ,  $\psi$  and  $\omega_n$  should remain constant, even if the static force changes. From Table 1, it follows that if the resistance  $R$  does not change, this is almost automatically obtained for the FAV system as soon as the pressure is adapted (with an external pump) to the new load, while for the BPR, both pressures need to be adjusted proportionally.

## 5. Design process

It is worth to take as a reference a traditional passive system composed by a metal spring and an oil damper. The simpler linear quarter-car model of this kind of system is:

$$\frac{\bar{z}}{\bar{u}} = \frac{2\zeta\omega_{nP}\mathbf{s} + \omega_{nP}^2}{\mathbf{s}^2 + 2\zeta\omega_{nP}\mathbf{s} + \omega_{nP}^2}, \quad (34)$$

where  $\omega_{nP}$  is, as before, the ratio between static stiffness and mass for this passive system and  $\zeta$  is its damping ratio. Generally, some good reference values are  $\zeta = 0.35$  and  $\omega_n = 1.4$  Hz [12].

To size both suspensions, a mass of 500 kg, acting on a single wheel, will be considered, thus corresponding to a static force  $F_0 = 4905$  N. Even if higher pressure means smaller device, there are practical limits and there is also a minimum stroke requirement for the suspension. As a consequence, the initial absolute pressure will be fixed to 6 bar and the semi-stroke of the cylinders to 10 cm. The temperature  $T_0$  used in the following calculations is 293 K.

### 5.1. By-pass resistance

The limit on the semi-stroke of the spring leads to a value for  $\omega_{nB}$  of:

$$\omega_{nB} = \sqrt{\frac{\gamma A_S^2 P_{S0}}{M V_{S0}}} \simeq \sqrt{\frac{\gamma A_S F_0}{M V_{S0}}} = \sqrt{\frac{\gamma A_S M g}{M A_S h_S}} = \sqrt{\frac{\gamma g}{h_S}} \simeq 12 \text{ rad s}^{-1}. \quad (35)$$

This will also leads to a maximum frequency allowed for  $\omega_{\chi^*} = \chi^* \cdot \omega_{nB}$  (Equation (32)):

$$\omega_{\chi^*} = \omega_{nB} \sqrt{\frac{2\lambda}{\lambda + 1}} = \sqrt{2}\omega_{nB} \sqrt{\frac{\lambda}{\lambda + 1}} \xrightarrow{\lambda \gg 1} \sqrt{2}\omega_{nB} \simeq 17 \text{ rad s}^{-1}. \quad (36)$$

This maximum frequency is not a problem for a normal vehicular application, where the natural frequency is usually between 6.3 and 9.4 rad s<sup>-1</sup>. The dimensionless plot in Figure 10 shows clearly that increasing the distance between the two peaks, do not affect strongly the frequency of the intersection point ( $\chi^* \simeq \sqrt{2}$ ).

The required area  $A_S$  is:

$$A_S = \frac{F_0}{P_{S0} - P_{\text{atm}}} = 0.00981 \text{ m}^2. \quad (37)$$

Choosing a resonant frequency of the optimal suspension of  $\omega_{\chi^*} = 8.8$  rad s<sup>-1</sup> and the maximum amplification  $H^* = 1.4$ , which means  $\lambda = 6$ , the value of  $\omega_{nB}$  can be found as a

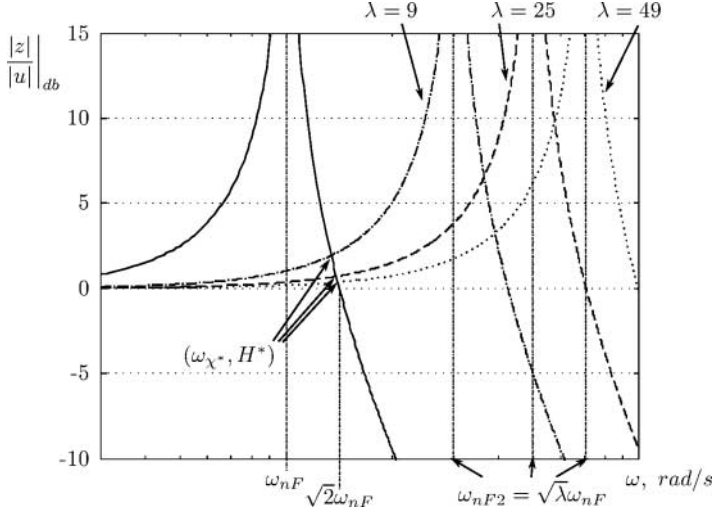


Figure 10. Intersection point  $(\omega_{\chi^*}, H^*)$ .

consequence:

$$\omega_{nB} = \omega_{\chi^*} \sqrt{\frac{\lambda + 1}{2\lambda}} = 6.72 \text{ rad s}^{-1}, \quad (38)$$

which is compatible with the maximum  $\omega_{nB}$  calculated in Equation (35). The volume of the spring follows from the expression of  $\omega_{nB}$  in Table 1:

$$V_{S0} = \frac{\gamma A_S^2 P_{S0}}{M \omega_{nB}^2} = 0.0036 \text{ m}^3. \quad (39)$$

The resulting stroke is  $h_S = V_{S0}/A_S = 37 \text{ cm}$ ; however, since only 10 cm of the stroke is necessary, the remaining volume can be arranged close to the cylinder in order to obtain a more compact solution. For what concerning the damper, given the desired stroke  $h_D$ , the already calculated  $\lambda$ ,  $A_S$  and  $V_{S0}$  and considering  $P_{S0} = P_{D0}$ , the required area comes from the expression of  $\lambda$  in Table 1:

$$A_D = \frac{h_D A_S^2 (\lambda - 1)}{2 V_{S0}} = 0.0067 \text{ m}^2. \quad (40)$$

It is convenient to chose the minimum allowed  $h_D = 10 \text{ cm}$  in order to obtain a less bulky damper. Since the volume is  $V_{D0} = A_D h_D = 6.72 \cdot 10^{-4} \text{ m}^3$ , the resistance  $R$  comes from the expression of  $\psi$ :

$$R = \frac{2\psi^* \gamma R_g T_0}{V_{D0} \omega_{nB}} = 1.63 \cdot 10^7 \text{ Pa kg}^{-1}. \quad (41)$$

## 5.2. Fixed auxiliary volume

For an FAV suspension, the minimum stroke of 10 cm again limits the natural frequency of spring alone ( $\omega_{nF2} = \sqrt{k_S/M} = \sqrt{\lambda} \cdot \omega_{nF}$ ). This is the natural frequency of the system when  $\psi = \infty$  (Figure 9):

$$\omega_{nF2} \simeq \sqrt{\frac{\gamma g}{h_S}} \simeq 12 \text{ rad s}^{-1}. \quad (42)$$

The first consideration is that, since  $\omega_{\chi^*} < \omega_{nF2}$ , an FAV system has a lower maximum limit on the peak transmissibility frequency  $\omega_{\chi^*}$ . However, to limit the size of the suspension, it is

convenient to use the minimum value of  $h_S$  and so the maximum value of  $\omega_{nF2}$ . The second important consideration is that, contrary to BPR, given the desired maximum amplification  $H^* = 1.4$  ( $\lambda = 6$ ), the frequency  $\omega_{\chi^*}$  is a consequence:

$$\omega_{\chi^*} = \omega_{nF} \sqrt{\frac{2\lambda}{\lambda + 1}} = 6.86 \text{ rad s}^{-1}. \quad (43)$$

It is important to notice that, to achieve a greater value of  $\omega_{\chi^*}$ , a smaller  $\lambda$  needs to be used, since the two are not independent. In fact, imposing  $\omega_{\chi^*} = 8.8 \text{ rad s}^{-1}$  as in BPR results in  $\lambda = 2.74$  and so to an unacceptable maximum amplification of  $H^* = 2.16$ . Anyway, the area is:

$$A_S = \frac{F_0}{P_{S0} - P_{\text{atm}}} = 0.00981 \text{ m}^2. \quad (44)$$

The spring volume is thus  $V_{S0} = h_S A_S = 9.8 \cdot 10^{-4} \text{ m}^3$ , while the auxiliary volume is:

$$V_{A0} = (\lambda - 1) V_{S0} = 0.005 \text{ m}^3. \quad (45)$$

Finally, the value of the resistance  $R$  can be obtained:

$$R = \frac{\gamma R_g T_0 \lambda \psi^*}{V_{A0} \omega_{nF}} = 8.57 \cdot 10^6 \text{ s Pa kg}^{-1}. \quad (46)$$

Depending on the type of resistance chosen (pipe or orifice), this will lead to specific geometric conditions.

Figure 11 shows the behaviour of the sized BPR and FAV suspensions along with the traditional suspension reference. It is clear how both suspensions are able to reduce the maximum amplification; however, while with BPR, it is possible to choose the resonant frequency, with FAV this is not possible, leading to a small crossover frequency. With BPR instead, it is possible to have a greater crossover frequency but to still attenuate better than a traditional solution at the higher frequency of interest.

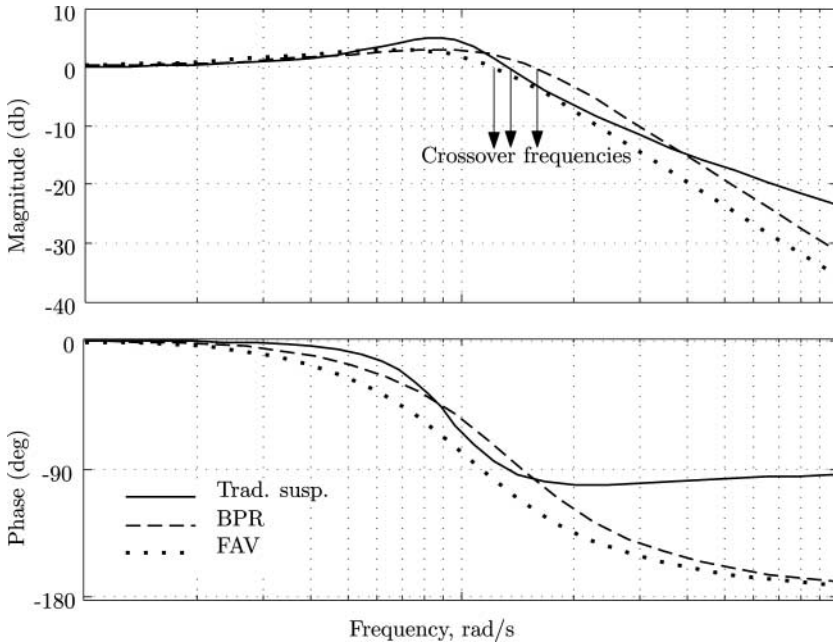


Figure 11. Comparison between a traditional, BPR and FAV suspensions.



### 5.3. Changes to the static pressure and to the temperature

The mathematical models used in this work are widely spread in all literature regarding air suspensions. However, they do not take into account the heating of the system due to the damping effect; in fact, the mean temperature of the air in a real plant, will likely increase, because part of the energy dissipated by the resistance will remain in the system itself as internal energy (heated air).

For an FAV system, an increase in the air temperature will lead to a volume expansion, since the pressure is fixed by the load, and so to a bigger static height: to overcome this issue, some air needs to be discharged. Anyway, this temperature increase will lead to a smaller value of  $\psi$  compared with the design value.

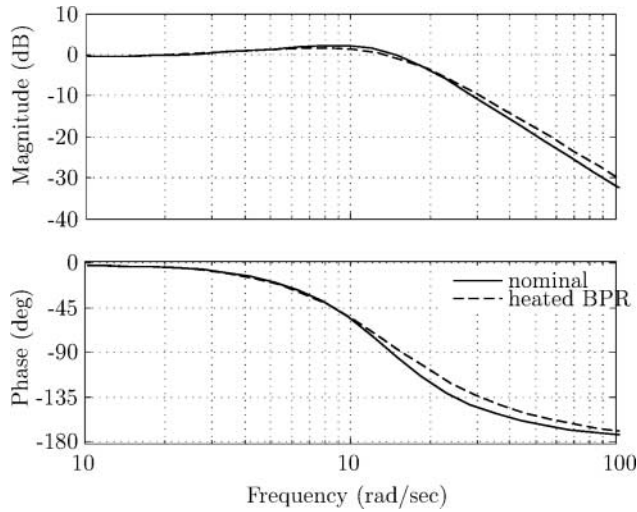


Figure 12. Effect of temperature rise (393 K) for both BPR and FAV.

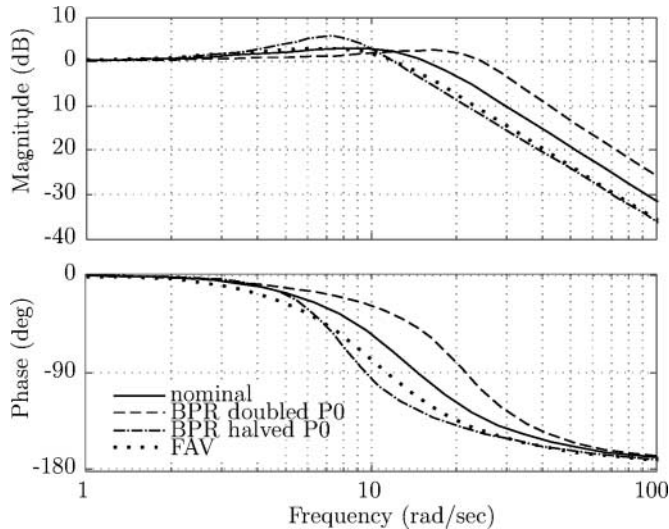


Figure 13. Effects of pressure change for BPR.

For a BPR, instead, only the temperature in the damping cylinder is likely to increase, leading also to a pressure rise because the volume is constant: this means that the static height remains constant.

As a consequence, it is clear that the two systems, after the initial transient, will probably behave differently in a real environment. Figure 12 shows, as an example, the nominal behaviour of the designed BPR suspension at the nominal temperature of 293 K and at 393 K: even with an heating of 100 K, the response of the system is close to the nominal.

Apart from temperature matters, with a BPR suspension, it is possible to change the pressure  $P_{D0}$  without affecting the static height. Figure 13 shows that, doubling  $P_{D0}$ , the natural frequency becomes greater leading to a stiffer vehicle. On the other hand, halving the pressure leads to an increased magnifications at low frequencies but to a stronger attenuation for higher ones (similar to the designed FAV system): this characteristic could be used to filter particular uneven road surfaces. It is worth noticing that, since the volume of the damping cylinder is little, it is relatively fast to change its pressure without involving a big power demand.

## 6. Conclusions

In this work, a linear dimensionless model which holds for two types of air suspensions (FAV and BPR) has been developed. It has shown that the BPR suspension system has some clear advantages over FAV in term of design degrees of freedom. Moreover, its behaviour can be adjusted between a stiff or a soft one, simply by changing the air pressure inside a small volume, without using additional devices to change the resistance.

Apart from this, the damping cylinder could be used simply coupled to a metallic spring, instead of an air spring, if there is no need to control the static height. This way, the nominal behaviour is the same as that of the air suspension shown in Figure 11 but, changing the sprung mass the system, it is no more isofrequency, like a traditional system.

Finally, even if there is yet any experimental validation, these kinds of models have been widely used and validated in the past decades.

## Nomenclature

$A$	area of the piston ( $\text{m}^2$ )
$F$	force (N)
$G$	mass flow rate ( $\text{kg s}^{-1}$ )
$h$	cylinder's semi-stroke (m)
$k$	stiffness ( $\text{N m}^{-1}$ )
$M$	quarter-car mass (kg)
$P$	absolute pressure (Pa)
$R$	linear fluidic resistance ( $\text{s Pa kg}^{-1}$ )
$T$	absolute temperature (K)
$V$	volume ( $\text{m}^3$ )
$u, x, y, z$	reference systems (m)
$\rho$	density ( $\text{kg m}^{-3}$ )
$\omega$	frequency ( $\text{rad s}^{-1}$ )
$\chi$	dimensionless frequency (—)

### Subscripts

0	initial value
A	FAV's auxiliary volume

atm	atmospheric conditions
DA, DB	chambers of the BPR's damping actuator
S	pneumatic spring

#### Constants

$R_g$	specific gas constant for dry air ( $287.05 \text{ J kg}^{-1} \text{ K}^{-1}$ )
$\gamma$	specific heat ratio (1.4)

A bar over a variable (ex.  $\bar{P}$ ) is the Laplace operator while  $s$  is the Laplace variable.

#### References

- [1] E.M. Elbeheiry, D.C. Karnopp, M.E. Elaraby, and A.M. Abdelraaouf, *Advanced ground vehicle suspension systems – a classified bibliography*, Veh. Syst. Dyn. 24 (1995), pp. 231–258.
- [2] Volkswagen, *Self-Study Programme 275 The Phaeton Air Suspension with Controlled Damping*, Volkswagen, 2003.
- [3] Audi, *Self-Study Programme 242 Pneumatic Suspension System Part 1 Selflevelling Suspension in the Audi A6*, Audi, 2001.
- [4] C. Hilgers, J. Brandes, D.H. Ilias, H. Oldenettel, D.A. Stiller, and C. Treder, *Active air spring suspension for greater range between adjusting for comfort and dynamic driving*, ATZ Worldwide, 111 (2009), pp. 12–17.
- [5] R.D. Cavanaugh, *Air suspension and servo-controlled isolation systems*, in *Shock and Vibration Handbook*, Vol. 2, C.M. Harris and C.E. Crede, eds., McGraw-Hill, New York, 1961, pp. 33.1–33.35.
- [6] E. Esmailzadeh, *Optimization of pneumatic vibration isolation system for vehicle suspension*, Trans. ASME. J. Mech. Des. 100 (1978), pp. 500–506.
- [7] A.J. Nieto, A.L. Morales, A. Gonzalez, J.M. Chicharro, and P. Pintado, *An analytical model of pneumatic suspensions based on an experimental characterization*, J. Sound Vib. 313 (2008), pp. 290–307.
- [8] K. Toyofuku, C. Yamada, T. Kagawa, and T. Fujita, *Study on dynamic characteristic analysis of air spring with auxiliary chamber*, JSAE Rev. (Soc. Automot. Eng. Jpn.) 20 (1999), pp. 349–355.
- [9] G. Quaglia and M. Sorli, *Air suspension dimensionless analysis and design procedure*, Veh. Syst. Dyn. 35 (2001), pp. 443–475.
- [10] F. Barecke, R. Kasper, and M. Al-Wahab, *A structured piezo ceramic mechatronic valve for an adaptive car gas damping system*, Proceeding of the 5th International Symposium on Mechatronics and its Applications (ISMA08), 27–29 May, Amman, Jordan, 2008.
- [11] P. Beater, *Some results from fluid mechanics*, in *Pneumatic Drives*, Chap. 4, Springer, Berlin, 2006, pp. 25–39.
- [12] D. Bastow and G. Howard, *Suspension systems and their effects*, in *Car Suspension and Handling*, Society of Automotive Engineers, Pentech Press, London, 1993, pp. 29–54.